Collaborative project

Small or medium-scale focused research project

THEME FP7-ICT-2009-4

Deliverable 2.2 - Evaluation and testing of switching behaviour of diodes based on blend and imprinted P(VDF-TrFE) layer

Contract no.:	248092
Project acronym:	MOMA
Project full title:	Embedded Organic Memory Arrays
Project website:	http://www.moma-project.eu

Coordinator contact details: Gerwin Gelinck (gerwin.gelinck@tno.nl)
TNO / Holst Centre
High tech Campus 31
PO Box 8550
5605KN Eindhoven
The Netherlands
Tel: +31 40 277 4098
Fax: +31 40 274 6400

Document revision history

Version	Date	Author	Summary of main changes
V1	16-06-2011	D.M. de Leeuw	First draft
V2	17-06-2011	G.H. Gelinck/A. van Breemen	Different introduction and other parts added
V3	22-06-2011	L. Nougaret/A. Jonas	Addition of Chapter 4 on imprinting
V4	31-07-2011	A. van Breemen	New TNO/UCL results added
V5	10-08-2011	Gerwin Gelinck	Third version sent to partners for approval
	15-08-2011	Gerwin Gelinck	Final version sent to Commission

Table of Contents:

1. Introduction

The main objective of WP2 is to develop all single devices that are necessary for the setup of the demonstrators in the project. Two-terminal as well as three-terminal memories will be explored. This deliverable deals with two terminal non-volatile memories using a ferroelectric polymer and a semiconducting polymer. The ferroelectric polymer provides the binary state and data retention, whereas the semiconducting polymer provides the means to probe that state via an electrical signal.

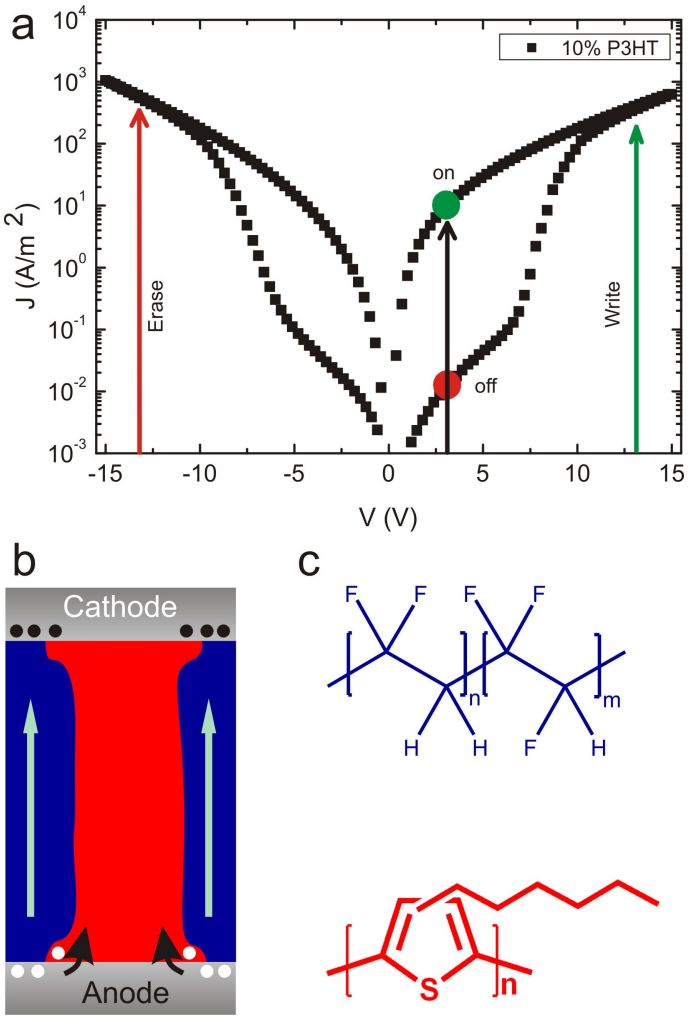

Figure 1. (a) J-V sweep of a typical polymer semiconductor / ferroelectric blend (10:90) diode demonstrating hysteresis in the conduction due to polarization of the ferroelectric phase. (b) Tentative operation mechanism. Polarization of the ferroelectric phase (blue) leads to accumulation of charges in the semiconductor domain (red) showing the low resistive state of the diode. (c) Structural formula of the chemical compounds used for this study P(VDF-TrFE) in blue and rir-P3HT in red.

RUG has demonstrated non-volatile memories based on phase separated blends of organic semiconductors and ferroelectrics. As a typical example we present in Figure 1 the current voltage characteristics of such a blend diode. The diode was made using a blend of 10 wt% semiconductor, viz. regio-irregular poly(3-hexylthiophene) (rir-P3HT), and 90 wt% of a

ferroelectric material, *viz.* the random copolymer poly(vinylidene fluoride-trifluoroethylene (P(VDF-TrFE)) (65 wt% PVDF, 35 wt% TrFE content). The chemical structures are presented in the inset. Figure 1a shows hysteresis in the electrical transport. The diode can be programmed into a high conductance ON-state and a low conductance OFF-state (current modulation of about 3 orders of magnitude) with writing and erasing taking place at fields larger than the coercive field of the ferroelectric. As a consequence, the diode can non-destructively be read out at low bias. The switching in such blend devices was attributed to changes in the charge injection at the electrode rir-P3HT contact. The tentative mechanism proposed is illustrated in Fig. 1b. Silver was used as an electrode yielding an injection barrier of 0.6-0.7 eV for which charge transport is injection limited. With such an injection barrier the current density in the diode is low corresponding to the OFF-state. The ferroelectric polymer polarizes in response to an applied voltage exceeding the coercive field. Figure 1b shows that a negative ferroelectric polarization is compensated for partially by charges in the silver electrode and partially by accumulation of holes in the semiconductor indicated as white circles in Figure 1b. As a consequence, the accumulated holes lead to strong band bending that lowers the injection barrier.

The switching in such blend devices was attributed to changes in the charge injection at the electrode rir-P3HT contact. The tentative mechanism proposed is illustrated in Figure 1b. Silver was used as an electrode yielding an injection barrier of 0.6-0.7 eV for which charge transport is injection limited. With such an injection barrier the current density in the diode is low corresponding to the OFF-state. The ferroelectric polymer polarizes in response to an applied voltage exceeding the coercive field. Figure 1b shows that a negative ferroelectric polarization is compensated for partially by charges in the silver electrode and partially by accumulation of holes in the semiconductor indicated as white circles in Figure 1b. As a consequence, the accumulated holes lead to strong band bending that lowers the injection barrier. The current through the diode then becomes space-charge limited corresponding to the ON-state.

In this report we present the electrical switching of discrete blend diodes as a function of composition (Chapter 2). In Chapter 3 we present current-sensing atomic force microscopy (c-AFM) measurements on a phase separated blend. Finally, in Chapter 4 we present the status of the nano-imprinting process of the P(VDF-TrFE) layer, and the realization of the first resistive switching diodes made with this process.

2. Electrical switching of discrete blend diodes as a function of composition

In this chapter we present the electrical switching of discrete blend diodes as a function of composition. The tentative interpretation of the switching mechanism is that the polarization field of the ferroelectric modulates the injection barrier at the metal-semiconductor contact. This implies that the phase separation should occur on a length comparable to the accumulation width of the semiconductor, which typically amounts to 10–20 nm. To resolve the mechanism we investigate scaling of the current transport with the domain size. The composition of the blends will be varied deliberately. The combination of detailed investigation of microstructure and charge transport will lead to an understanding of the switching mechanism including estimations for the injection barriers that can be tolerated, the current modulation that can be achieved, and the minimum feature size for a functional separated memory.

The random 65%-35% copolymer of P(VDF-TrFE) from Solvay was used as received. Regio-irregular (regiorandom) poly(3-hexyl thiophene) (rir-P3HT), was purchased from Rieke Metals, Inc. and chosen because of ease of processing and solubility in common solvents. Rir-P3HT was purified by dissolving in distilled toluene, dedoping with hydrazine and precipitating in methanol. The precipitate was Soxhlet extracted with methanol, n-hexane, and CH2Cl2 until the extraction solvent was colorless. The dichloromethane fraction was precipitated in methanol, collected, dissolved in chloroform and precipitated again in methanol. The collected fraction was dried under vacuum and stored in a glovebox under nitrogen. Solutions of 20-30 mg ml-1 in distilled THF were prepared by co-dissolving P(VDF-TrFE) and rir-P3HT. The mixing ratio of the two polymers rir-P3HT:P(VDF-TrFE) was varied from 0:100, to 1:99, 2:98, 3:97, 5:95, 10:90 and 20:80. After complete dissolution of the polymers, typically a few hours, the solution was filtered with 1µm PTFE filters. Clean glass slides, sonicated in acetone and propanol and dried in an oven, were used as substrates. We first deposited the bottom electrode consisting of 40 nm of gold or silver with 1 nm of chromium as adhesion layer via shadow masks in vacuum with a base pressure of $1\text{-}2\times10^{-6}$ mbar. Blend films were then spin-coated in a nitrogen-filled glove box. The thickness of the film was measured with a DEKTAK profilometer and varied between 120-200 nm. The films were annealed in a vacuum oven at 140 ºC for two hours with slow heating and cooling rate. Resistive switching diodes were finished with evaporation of 70 to 100 nm of silver top electrodes. The current-voltage measurements were conducted in vacuum, 1×10^{-6} mbar with a Keithley 4200 Semiconductor Characterization System or Keithley 2400 Source Meter. Ferroelectric characterizations were done either by constructing Sawyer-Tower circuit or by pulse technique using a ferroelectric characterization system (Radiant Technology). In the latter case, a pulse of known polarity is applied to set in a known polarization state. Subsequently two pulses of opposite polarity were applied and the responses were recorded. The response of the first pulse contains information about the switching plus the non-switching currents whereas the second pulse gives the non-switching current of the device. Subtracting the two responses gives the net switching current. Remnant polarization was determined by integration of the net switching current in time.

To probe the ferroelectric properties of the blends we used two common techniques e.g. a Sawyer-Tower circuit and transient pulse measurements. Electric displacement loops versus electric field for neat P(VDF-TrFE) capacitors gave a coercive field of nearly 50 MV/m. The remnant polarization amounted to 60-70 mC/m^2 in good agreement with literature values. The displacement loop measured for the blend capacitors however is distorted. The presence of rir-P3HT in the matrix increases the leakage current. Measuring the polarization therefore results in unrealistic and unphysical values for the remnant polarization. We thus carefully studied the remnant polarization by a pulse technique that compensates for leakage currents. The polarization as a function of blending ratio is presented in Figure 2 which shows that

ferroelectricity is maintained in the blend, and that the remnant polarization scales linearly with the rir-P3HT content with an slope of ±0.17 μC cm^{-2} [rir-P3HT]$^{-1}$.

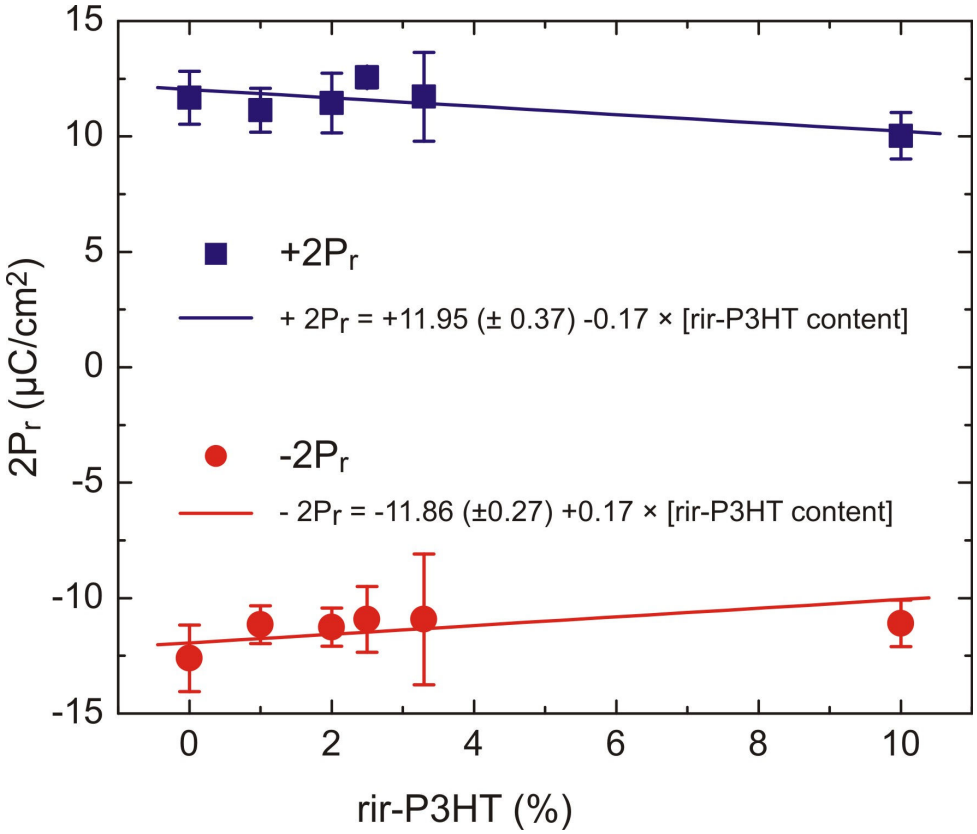

Figure 2. Remnant polarization of rir-P3HT:P(VDF-TrFE) blends as a function of rir-P3HT content.

The current density in the OFF-state is injection limited. For the present diodes it is about equal to the parasitic leakage current. Hence to evaluate the switching behavior we focused on the ON-state current density. The current at high bias is space charge limited, indicating that the injection barrier due to the gold processing is small. The current density for each vertical diode was determined at low field, compensated for the thickness, and presented on a semi-logarithmic scale in Figure 3 as a function of rir-P3HT content. For comparison both data sets, silver and gold, are presented in the same graph. Neat rir-P3HT is included as a reference. Up to 10 w% the spread in current density for each blend ratio is small. At higher ratios the spread increases up to about an order of magnitude. The current density for gold was determined for pristine, unpoled diodes. For silver we present the current density of resistive switches in the ON-state. The current in the ON-state both poled up and down are similar, indicating that the silver bottom contact and silver top contact are identical.

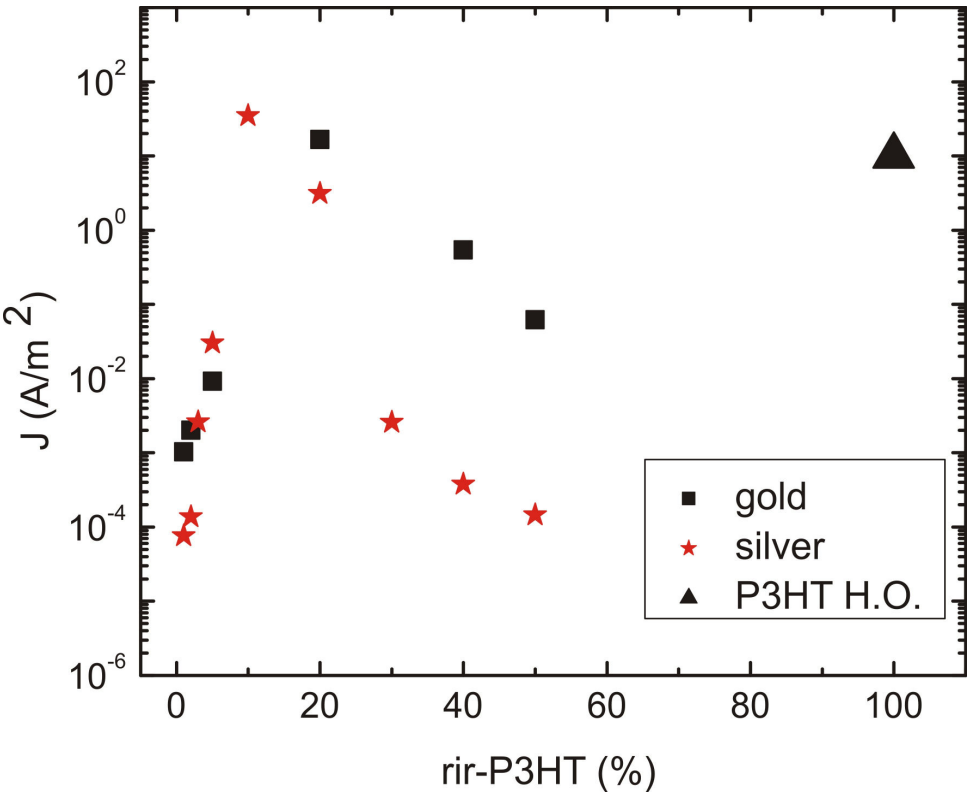

Figure 3. Current density at an electric field of 20 MV/m for vertical blend diodes with both gold electrode (square) and both silver (star) electrodes. Triangle shows space charge limited current density for a hole only rir-P3HT diode at the same electric field.

To interpret the measurements we first discuss what is expected in zero order approximation. Gold is an almost Ohmic contact and the current density therefore should scale linearly with rir-P3HT content. Figure 3 shows that at low P3HT content the current density increases but that the current density at high weight content counterintuitively decreases. The origin is not understood. To interpret the electrical transport of diodes with silver electrodes we approximate the morphology by taking the rir-P3HT domains as identical cylindrical columns that are continuous through the film from the bottom contact to the blend air interface. Upon poling charges are accumulated at the circumference of the semiconducting domain; the band bending then eliminates the injection barrier. We take a characteristic length scale for the average accumulation width. This length, *L*, is independent of domain size and taken equal for all blend compositions. At low rir-P3HT content, when the accumulation length is larger than the domain radius, the whole domain contributes to the injection and transport. The current density in the ON-state then should be identical to that of the diodes with Ohmic gold contacts, as experimentally verified. At some critical semiconductor content, the accumulation width becomes equal to the domain radius, *r*. For rir-P3HT content above this critical threshold the injection and current density in first order approximation should then scale with $\square L^2/(2r/L-1)$. We note that for both high and low P3HT content the current density should depends linearly on P3HT content. Experimentally however an almost exponential relation is observed. The origin is not yet understood. We note that the maximum current density in the ON-state for all diodes occurs at about 10 w% P3HT. This indicates that the characteristic length scale of charge accumulation is around 200 nm. In first order approximation we had expected an characteristic length scale comparable to the thickness of the accumulation layer in a field-effect transistor, *viz.* at most 10 nm. The present estimation is significantly larger. The discrepancies might be due to details in the microstructure. The rir-P3HT domains are not perfect cylinders. The blend films coarsen with increasing rir-P3HT content. The roughness then becomes even comparable to the layer thickness. Optimization of the processing technology is

required to arrive at a quantitative interpretation of the current densities and the accumulation length.

In summary, the current perpendicular through the film was measured using both Au and Ag electrodes as a function of blend composition. For Ohmic Au electrodes the space charge limited current density increases with rir-P3HT content upto about 10 w%, albeit exponential rather than linear as expected. At higher content the current density is expected to be similar to a rir-P3HT only diode. Experimentally much lower current densities have been obtained. The reason could be related to the details of the microstructure but is not yet fully understood. For Ag diodes at low rir-P3HT content and poled into the ON-state, the current density is similar to the corresponding Au diodes, demonstrating that the injection barrier has disappeared and that the whole domain contributes to the charge transport. For larger rir-P3HT content the Ag ON-state current density is significantly lower than that of the corresponding Au diodes. The injection occurs at the circumference of the domains. From the measurements we estimate an accumulation width over which the injection occurs in the order of a few hundred nm.

3. Current-sensing AFM measurements

Current-Sensing Atomic Force Microscopy (CS-AFM) is a powerful technique for electrical characterization of conductivity variation in resistive samples. It allows direct and simultaneous visualization of the topography and current distribution of a sample. The CS-AFM technique needs cantilevers coated with a conducting film, which operate in the standard AFM contact mode. Applying a voltage bias between the substrate and conducting cantilever generates a current flow. The current can be used to construct a spatially resolved conductivity image. The image is formed for a constant voltage bias and a constant cantilever load. The current image and sample topography are recorded simultaneously. Changing the bias voltage controls the contrast in the current image. Point current-voltage (*I-V*) characteristics can be measured during scanning the probed surface area for a programmed net of measurement points.
In this report the CS-AFM technique has been implemented to study locally the flow of charge carriers in a blend of P(VDF-TrFE) and Poly(9,9'-dioctylfluorene) (PFO) from the bottom (ITO) to a top electrode (here, the Pt tip of the AFM). A schematic picture of the CS-AFM set-up is depicted in Figure 4. The AFM scanned the surface of the sample in contact mode. A set point voltage of -0.2V is applied in order to maintain the contact force constant. The conductive tip was grounded and a DC bias was applied to the sample via the bottom electrode (0-10V). The range of the current values changes between 10 pA and 10 nA (below 10pA it is noisy).

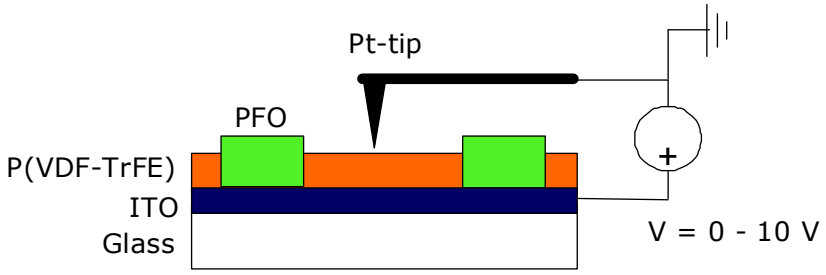

Figure 4. Schematic picture of current sensing AFM set-up.

Poly(9,9'-dioctyl-fluorene) (PFO) (M_w = 99 kDa, D = 3.0) was synthesized by TNO according to a modified Suzuki-polymerization.[1,2] Poly(vinylidene fluoride-*co*-trifluoroethylene) (P(VDF-TrFE)) (M_w = 220 kDa, 2.3 < D < 2.8 with a 77/23 VDF/TrFE mole ratio) was supplied by Solvay and used as received. The blend solution (2.5 wt% of 1:9 (w/w) PFO:P(VDF-TrFE) in cyclohexyl acetate (CHA)) was prepared by stirring the mixture over night at room temperature, followed by heating at 60 °C for 3h. Upon cooling a clear solution was obtained. The 1:9 weight ratio approximately corresponds to a 1:5 volume ratio, as $\rho_{P(VDF\text{-}TrFE)}/\rho_{PFO}$ ~1.8 g/cm^3. Layers of the polymer blend (d ~ 200 nm) were obtained by spin-coating the solution on cleaned glass-ITO substrates in a nitrogen filled glovebox. After a defined spinning time, the remainder of the solvent was flash-evaporated by placing the substrate on a hot plate equilibrated at 135 °C. Subsequently, the samples were annealed at 135 °C for 1h in the same glovebox.

The phase separation of a P(VDF-TrFE):PFO blend occurs by spinodal decomposition. This type of decomposition inherently yields rough surfaces. A typical example of an AFM topography image is shown in Figure 5a. It shows domains of semiconductor embedded in a ferrroelectric PVDF-TrFE matrix. The current image of the identical surface area is depicted in Figure 5b. The dark regions correspond to higher current points, whereas the white regions correspond to

[1] van Woudenbergh, T.; Wildeman, J.; Blom, P. W. M.; Bastiaansen, J. J. A. M.; Langeveld-Voss, B. M. W. *Adv. Func. Mater.* **2004**, *14*, 677-683.
[2] Miyaura, N.; Suzuki, A. *Chem. Rev.* **1995**, *96*, 2457.

lower current ones. When topography and current images are compared, we conclude that only about 80 % of the PFO domains are electrically active.

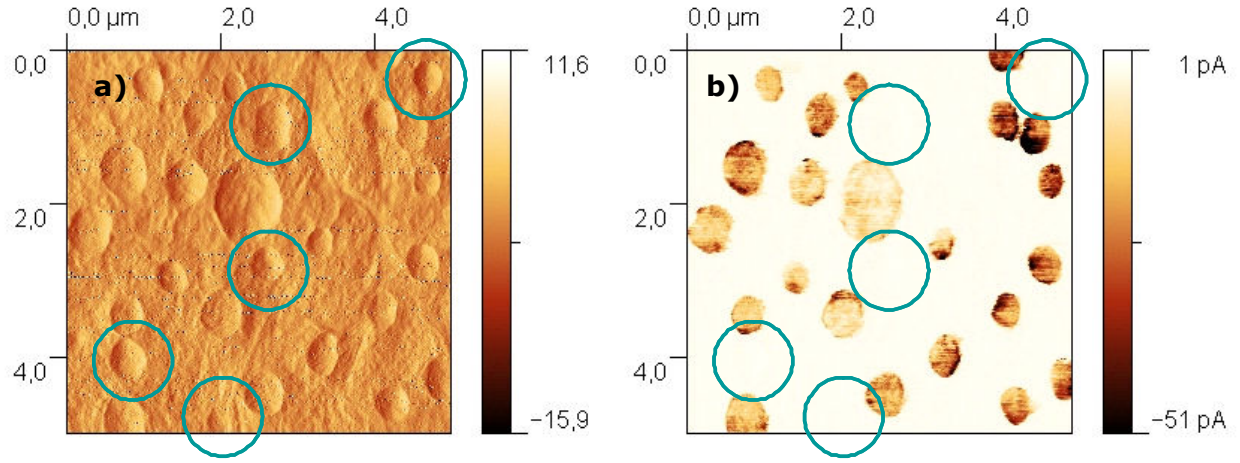

27 PFO domains **22 PFO domains "active"**

Figure 5: AFM images of a P(VDF-TrFE):PFO 9:1 blend with a scan area of 5x5 µm² a) topography and b) current sensing image of the identical surface area.

Initial modelling experiments of the phase separation of P(VDF-TrFE):PFO blends have shown that this inactivity might be due to a residual P(VDF-TrFE) layer underneath some PFO domains as can be seen in Figure 6.

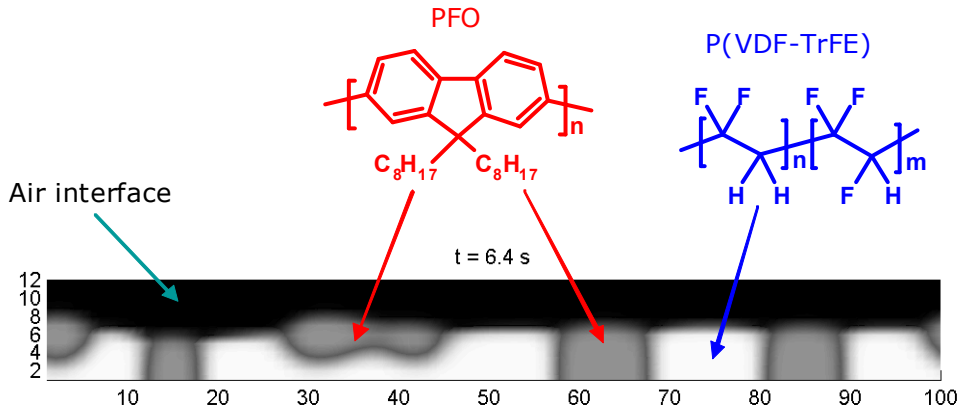

Figure 6: side-view of modelling result of P(VDF-TrFE):PFO blend. Some of the PFO domains do not fully percolate toward the substrate.

4. Resistive switching diodes based on imprinted P(VDF-TrFE) layers

In addition to blend diodes, we are exploring the possibility to fabricate diodes wherein the location of the semiconducting and ferroelectric components are controlled by nanoimprint lithography. The general concept is illustrated in Figure 7. Contrarily to the previous case where a phase separation process occurs in the active layer, here the ferroelectric layer is first spin-coated and shaped using molds bearing nanocavities (typical lateral size and depth are in the range 100-200 nm; the fill factor is close to 0.5). Then, the semiconducting layer is placed in the open trenches of the imprinted ferroelectric layer. This process should permit a better control over the morphology of the active layer, and offers possibilities for scaling-down the devices. In addition, it was shown previously that, when the imprinting is performed so as to effectively remove the residual layer between the protruding ferroelectric dots, the confinement which ensues results in an improved crystallinity of the ferroelectric polymer, a favorable orientation of the polar axis, and a significantly-decreased coercive field. This should help decrease the operating voltages of the devices. As regards the functioning of the memory diode, we assume that the current level flowing through the semiconducting component in the diode depends on the orientation of the permanent electric dipole moment of the ferroelectric nanodots, as was demonstrated for the blend diodes.

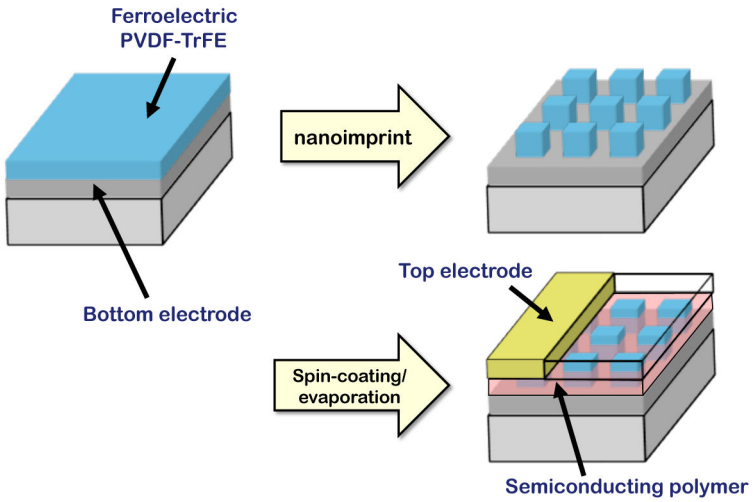

Figure 7. Scheme of the fabrication of a ferroelectric/semiconductor mixed diode by nanoimprint lithography.

The substrates were made of a 200 nm-thick thermal SiO_2 layer over a Si (100) wafer, over which a bottom electrode was deposited (different choices were made), followed by spin-coating of the PVDF-TrFE layer. The selected P(VDF-TrFE) was provided by Solvay Solexis. Different grades were tested for nanoimprinting in the paraelectric liquid crystalline phase, between the Curie point and the melting temperature; most of them gave adequate results provided the imprinting temperature was about 5-10°C below the melting temperature. Here, we report on devices fabricated with the SOLEF 05018TA1005 grade (70/30 w/w VDF/TrFE), which was selected to allow us to perform comparisons with results acquired in a previous research project. The moulds used for nanoimprint were fabricated by e-beam lithography and RIE plasma etching performed on Si wafers covered with a 200 nm-thick SiO_2 oxide layer. The active area of the mould, and the size and the depth of nanocavities are summarized in Table 1; the nanocavities are repeated over a simple square lattice. In order to decrease the adhesion of the moulds, they are covered by a perfluoroalkyltrichlorosilane monolayer. The typical imprinting conditions are 60 bar, 135°C, 10 min. As for the thickness of the starting

ferroelectric layer, it was adjusted so to make sure that no residual layer would exist after imprinting.

Mould name	Imprint area (mm^2)	Lateral size of cavities (nm)	Repeat period of the square lattice (nm)	depth of cavities (nm)
1	$2\ 10^{-3}$	250	350 nm	90
2 IEMN	4	207	288 nm	200
3 IEMN	4	100	143 nm	200

Table 1 : geometrical parameters of the moulds used to imprint the ferroelectric layer

The ferroelectric properties of the P(VDF-TrFE) nanodots were measured by piezoelectric force microscopy (PFM). Bulk (PVDF-TrFE) has a remnant polarization of about 90 mC/m^2 and a coercive field slightly higher than 50 MV/m. Local hysteresis loops were obtained by PFM, and it was confirmed that the coercive field was decreased compared to the bulk material. We are currently studying the extent of this decrease depending on the grade of the P(VDF-TrFE) and on the geometrical characteristics of the mould. In addition, we have studied by PFM the stability of the ferroelectric storage in the imprinted layer (Figure 8). The storage was found to be thermally-stable until the onset of the Curie transition of the bulk material, showing that the nanometer size of the ferroelectric nanodots does not affect thermal stability compared to the bulk material.

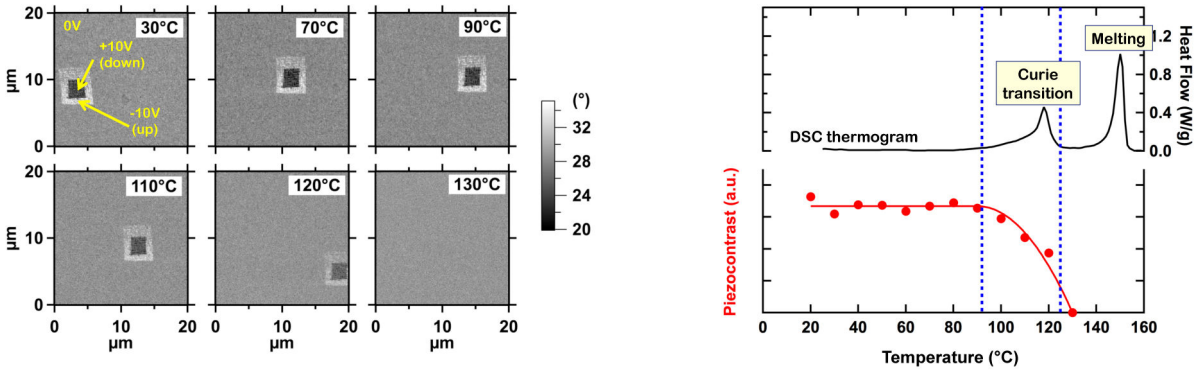

Figure 8. Stability of the ferroelectric storage in nanoimprinted P(VDF-TrFE). Left. PFM phase images of a region containing downward and upward pointing electric dipole moments, for different acquisition temperatures. Right. PFM contrast versus temperature for the nanoimprinted layer, and DSC thermogram of the same sample in the bulk phase.

After imprinting, the semiconducting (SC) layer is deposited by spin coating. We have investigated different SCs, spin-coated from toluene solutions : 1 wt% regio-irregular (rir) P3HT (from Sigma Aldrich), 0.5 wt% PFO (from TNO), 1.5 wt% PTAA (from TNO). In order to reproduce the features of the blend diodes, the top of the ferroelectric nanodots should be bare and in direct contact with the top electrode. This can be achieved by annealing the semiconducting layer in a solvent vapour (not affecting the P(VDF-TrFE) polymer), which promotes the displacement of the SC from the top of the P(VDF-TrFE) dots to the grooves separating them. An AFM topographic study of the displacement of the SC was performed versus annealing time, leading to an optimization of the initial SC thickness (20 nm if spin-coated over a flat surface) and of the vapour annealing time (~20 min).
The functioning of the blend diodes critically depends on the nature of the bottom and top electrodes. The same should hold true for the nanoimprinted diodes. Therefore, different electrodes were tested among the following : Pt, Pd, Ag, Au, PSS:PEDOT, for the three selected SCs. Depending on the specific combination electrode/semiconductor, the hole injection barrier

is smaller than 0.4eV (ohmic contact), is comprised between 0.7 and 1.2 eV (injecting contact), or is larger than 1.4 eV (blocking contact). In order to study the current modulation of the devices, we have used a DC probe station Agilent PSPM8 to obtain the I(V) curves. In parallel, we have used CS-AFM (current sensing atomic force microscopy) on systems devoid of top electrode to observe the local current modulation. In this case, the metal of the tip was chosen in order to have an ohmic contact with the semiconducting layer.
Among the different systems tested, essentially two provided promising results. The first system is a PSS:PEDOT / P3HT & P(VDF-TrFE) / Ag diode, shown in Figure 9. The PSS:PEDOT/P3HT interface should be ohmic, because the hole injection barrier between PSS:PEDOT and P3HT is ~0.0 eV. In contrast, a barrier of ~0.8 eV exists between Ag and P3HT. The current flowing from the Ag to the PSS:PEDOT electrode is modulated by the permanent dipole moment of P(VDF-TrFE); this is not the case for the current flowing from the PSS:PEDOT to the Ag electrode. The built-in potential between the PSS-PEDOT and Ag is 0.8 V corresponding to a depolarization field of ~20 MV/m. This might be the reason why the current is quite low below ~1 V.

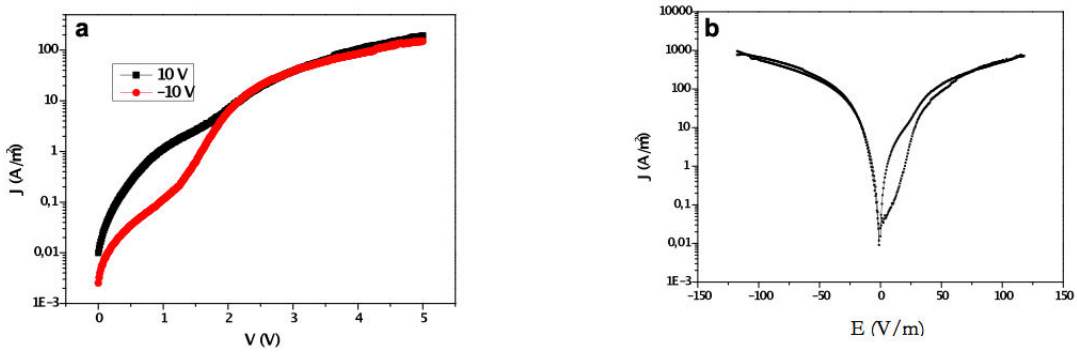

Figure 9: a) Current density versus voltage for a nanoimprinted device initially poled at +10 or -10 V (the bottom electrode, which is PSS:PEDOT, is grounded; the top electrode is Ag; the height of the PVDF-TrFE nanodots is 80 nm; the semiconductor is P3HT). b) Hysteresis loop of the current density versus electrical field. The PSS:PEDOT electrode is grounded.

The second system showing a modulation of current depending on the polarization of the P(VDF-TrFE) nanodots is an Au / PFO & P(VDF-TrFE) / Pt diode. PFO has a HOMO level around 5.9-6.1 eV. The Pt/PFO contact is close to ohmic (~0.5 eV) whereas the PFO/Au contact is slightly injecting (1.2 eV). The built-in potential is ~0.7 V. Figure 10 presents the I(V) hysteresis loop of this system. The current flowing in the system from Au to Pt is modulated by the polarization of the ferroelectrics, whereas it is not when flowing from Pt to Au.

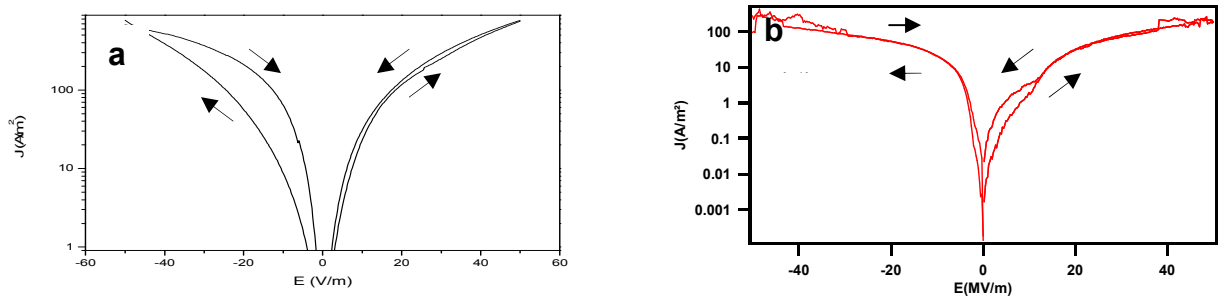

Figure 10: a) Hysteresis loop of the current density versus electrical field (bottom electrode Au is grounded; the top electrode is Pt; the height of the PVDF-TrFE nanodots reference sample is 200 nm; the semiconductor is PFO). b) Hysteresis loop of the current density versus electrical field (the bottom electrode, which is Ag, is grounded; the top electrode is Ag; the height of the PVDF-TrFE nanodots reference sample is 200 nm; the semiconductor is PFO).

All other probed systems either did not exhibit a modulation of current depending on poling, or gave very large values of current. This might be due to shortcuts between the bottom and top electrodes. A methodology of imprinting with softer moulds is currently being developed, to make sure that the bottom electrodes are not damaged by the process, and to decrease further adhesion problems. In addition, symmetric systems are being investigated, to separate better the role of each electrode in the modulation of current. An example is shown in Figure 10b, which displays the hysteresis loop of a symmetrical Ag/ PFO & P(VDF-TrFE) / Ag system. The PFO/Ag contact has a barrier for holes of 1.8 eV. The asymmetry results from the difference in oxidation and roughness of the top and bottom electrodes; the modulation is very small, if any. In summary, the results displayed in Figure 9 and Figure 10 indicate that nanoimprinted diodes might be a viable alternative to phase-separated diodes, provided the fabrication process and control parameters be fully understood. This requires more research performed in a systematic way on symmetrical systems, which will be performed in coming months.